

# Aberrant GABA<sub>A</sub> Receptor Expression in the Dentate Gyrus of the Epileptic Mutant Mouse Stargazer

Helen L. Payne,<sup>1</sup> Peter S. Donoghue,<sup>1</sup> William M. K. Connelly,<sup>2</sup> Sabine Hinterreiter,<sup>3,4</sup> Priyanka Tiwari,<sup>1</sup> Jane H. Ives,<sup>1</sup> Victoria Hann,<sup>1</sup> Werner Sieghart,<sup>3,4</sup> George Lees,<sup>2</sup> and Christopher L. Thompson<sup>1</sup>

<sup>1</sup>School of Biological and Biomedical Sciences, Science Research Laboratories, Durham University, Durham DH1 3LE, United Kingdom, <sup>2</sup>Department of Pharmacology and Toxicology, Otago School of Medical Sciences, University of Otago, Dunedin, New Zealand, <sup>3</sup>Centre for Brain Research, Medical University Vienna, A-1090 Vienna, Austria, and <sup>4</sup>Section for Biochemical Psychiatry, University Clinic for Psychiatry, A-1090 Vienna, Austria

Stargazer (*stg*) mutant mice fail to express stargazin [transmembrane AMPA receptor regulatory protein  $\gamma 2$  (TARP $\gamma 2$ )] and consequently experience absence seizure-like thalamocortical spike-wave discharges that pervade the hippocampal formation via the dentate gyrus (DG). As in other seizure models, the dentate granule cells of *stg* develop elaborate reentrant axon collaterals and transiently overexpress brain-derived neurotrophic factor. We investigated whether GABAergic parameters were affected by the *stg* mutation in this brain region. GABA<sub>A</sub> receptor (GABAR)  $\alpha 4$  and  $\beta 3$  subunits were consistently upregulated, GABAR  $\delta$  expression appeared to be variably reduced, whereas GABAR  $\alpha 1$ ,  $\beta 2$ , and  $\gamma 2$  subunits and the GABAR synaptic anchoring protein gephyrin were essentially unaffected. We established that the  $\alpha 4\beta\gamma 2$  subunit-containing, flunitrazepam-insensitive subtype of GABARs, not normally a significant GABAR in DG neurons, was strongly upregulated in *stg* DG, apparently arising at the expense of extrasynaptic  $\alpha 4\beta\delta$ -containing receptors. This change was associated with a reduction in neurosteroid-sensitive GABAR-mediated tonic current. This switch in GABAR subtypes was not reciprocated in the tottering mouse model of absence epilepsy implicating a unique, intrinsic adaptation of GABAergic networks in *stg*.

Contrary to previous reports that suggested that TARP $\gamma 2$  is expressed in the dentate, we find that TARP $\gamma 2$  was neither detected in *stg* nor control DG. We report that TARP $\gamma 8$  is the principal TARP isoform found in the DG and that its expression is compromised by the stargazer mutation. These effects on GABAergic parameters and TARP $\gamma 8$  expression are likely to arise as a consequence of failed expression of TARP $\gamma 2$  elsewhere in the brain, resulting in hyperexcitable inputs to the dentate.

**Key words:** hippocampus; stargazin; TARPs; AMPA receptors; GABA<sub>A</sub> receptors; absence epilepsy

## Introduction

The stargazer (*stg*) mutant mouse arose by a spontaneous viral transposon insertion into and subsequent premature transcriptional arrest of the stargazin gene (Letts et al., 1998). Thus, *stg* mice fail to express stargazin protein (Ives et al., 2004). Stargazin is a member of the family of transmembrane AMPA receptor (AMPA) regulatory proteins (TARPs) that are involved in AMPAR synaptic targeting and/or surface trafficking (Chen et al., 2000; Rouach et al., 2005). The TARPs ( $\gamma 2$ ,  $\gamma 3$ ,  $\gamma 4$ , and  $\gamma 8$ ), of which stargazin is TARP $\gamma 2$ , are expressed in the brain in a temporal spatially regulated manner, with some brain areas and possibly single cells expressing multiple TARP isoforms (Tomita et al., 2003). TARP $\gamma 2$  is reported to be heavily expressed in the cerebellum and moderately so in hippocampus (CA3 and den-

tate), cerebral cortex, thalamus, and olfactory bulb (Sharp et al., 2001; Tomita et al., 2003). In the cerebellum, the consequences of the stargazer mutation are primarily restricted to the cerebellar granule cells (CGCs), neurons that normally only express the TARP $\gamma 2$  isoform. Consequently, mossy fiber–CGC synapses in *stg* are bereft of AMPARs and are subsequently electrically silent (Chen et al., 2000), leading to a CGC-specific deficit in brain-derived neurotrophic factor (BDNF) expression and signaling (Qiao et al., 1998). Paradoxically, neurons in the dentate of the hippocampal formation in *stg* experience spontaneous nonconvulsive bilaterally symmetrical 6–7 Hz spike-wave discharges (SWDs) (Chafetz et al., 1995), intense mossy fiber sprouting, and intermittent elevations of BDNF expression but without extensive cell injury (Qiao and Noebels, 1993b; Chafetz et al., 1995; Nahm and Noebels, 1998). This contrasts with convulsive seizure activity, which results in significant cell death in CA1/CA3 and hilar cells of the dentate gyrus (DG) (Leroy et al., 2004). Chronic depolarization of dentate granule cells after convulsive seizures mediates an apparent adaptive modification of their inhibitory potential, presumably to titrate the increased network excitability. Such adaptations include modified GABA<sub>A</sub> receptor (GABAR) subunit expression and subtype assembly, resulting in altered GABAR function, pharmacology, targeting, and clustering (Clark 1998; Nusser et al., 1998; Elmariah et al., 2004; Leroy

Received Nov. 30, 2005; revised June 15, 2006; accepted July 6, 2006.

This work was funded by Wellcome Trust Grants 0543478 and 066204, Biotechnology and Biological Sciences Research Council Grant BBS/B/09899, and Austrian Science Fund Grant P17203. H.L.P. was supported in part by Merck Sharp and Dohme, and P.S.D. was supported by the Institut de Recherches Servier. We thank Dr. Dane Chetkovich (Northwestern University, Chicago, IL) for TARP $\gamma 3$ , TARP $\gamma 4$ , and TARP $\gamma 8$  cDNAs, and Andrew Crawford for Figure 1 E and Simon Kaja (Departments of Neurology and Neurophysiology, Leiden University Medical Centre, Leiden, The Netherlands) for critical reading of this manuscript.

Correspondence should be addressed to Dr. Christopher L. Thompson, School of Biological and Biomedical Sciences, Durham University, Science Research Laboratories, South Road, Durham DH1 3LE, UK. E-mail: c.l.thompson@durham.ac.uk.  
DOI:10.1523/JNEUROSCI.1088-06.2006

Copyright © 2006 Society for Neuroscience 0270-6474/06/268600-09\$15.00/0

et al., 2004). Whether GABAR plasticity is also induced in the *stg* DG by nonconvulsive SWDs has not been investigated. We have shown previously that neuronal GABAR expression *in vitro* is influenced by electrical activity (Ives et al., 2002), corroborated by our observations in electrically silent CGCs in *stg in vivo* (Thompson et al., 1998) in which GABAR  $\alpha 6$  and  $\beta 3$  subunits and the flunitrazepam-insensitive (BZ-IS) subtype of GABAR were downregulated. Because electrical activity and BDNF expression is decreased in CGCs, although paradoxically increased in the DG of *stg*, we hypothesized that GABAR expression may be reciprocally compromised in the DG. Here we show that GABAR subtypes expressed in the DG of *stg* are rearranged by a mechanism that is not directly related to the stargazer mutation because we show that the dentate does not normally express TARP $\gamma 2$ . Furthermore, these specific GABAR rearrangements are not a common feature of absence epileptic phenotypes because they are not reciprocated in tottering (*tg*) mutant mice, indicating that a unique mechanism underpins this form of GABAR plasticity.

## Materials and Methods

**Materials.** Anti-GABAR  $\alpha 4$ (1–14),  $\beta 3$ L(345–408),  $\gamma 2$ (319–366), and  $\delta$ (1–44) subunit-specific antibodies were as described previously (Sperk et al., 1997). Anti-GABAR  $\alpha 1$ (Cys1–15) antibody was a gift from Professor F. Anne Stephenson (School of Pharmacy, London, UK). Affinity-purified anti-NMDA NR1, extreme C-terminus-directed anti-TARP $\gamma 2$  antibody (Ives et al., 2004), and N-terminus-directed anti-TARP $\gamma 8$  antibodies (peptide sequence Cys1–14; MESLKRWNEERGLWC) were produced as described previously (Thompson et al., 2002; Ives et al., 2004). Anti-glutamate receptor subtype 2 (GluR2) antibody was from Santa Cruz Biotechnology (Calne, Wiltshire, UK). Anti- $\beta$ -actin antibody was obtained from Sigma (Poole, UK). Anti-gephyrin antibody was obtained from Clontech (Cowley, Oxford, UK). Vectastain Elite ABC immunohistochemistry kits were purchased from Vector Laboratories (Peterborough, UK). Hyperfilm ECL, [<sup>3</sup>H]-sensitive autoradiography film, horseradish-peroxidase-linked anti-rabbit secondary antibodies, and [<sup>3</sup>H]flunitrazepam were purchased from Amersham Biosciences (Aylesbury, Bucks, UK). Horseradish-peroxidase-linked anti-goat secondary antibody was obtained from Pierce (Chester, Cheshire, UK). [<sup>3</sup>H]muscimol and [<sup>3</sup>H]Ro15-4513 (ethyl-8-azido-5,6-dihydro-5-methyl-6-oxo-4H-imidazo[1,5 $\alpha$ ][1,4]benzodiazepine-3-carboxylate) were purchased from PerkinElmer (Boston, MA). Flunitrazepam, 8-fluoro-5,6-dihydro-5-methyl-6-oxo-4H-imidazo[1,5 $\alpha$ ][1,4]benzodiazepine-3-carboxylate (flumazenil; and Ro15-1788), and Ro15-4513 were a gift from Hoffmann LaRoche (Basel, Switzerland).

**Animals.** Wild-type strain for stargazer (C3B6Fe+; +/+), heterozygous (C3B6Fe+; +/*stg*) and homozygous stargazer mutant mice (C3B6Fe+; *stg/stg*), and wild-type strain for tottering (C57/B6+/+) and tottering (C57/B6 *tg/tg*) were maintained on a 12 h light/dark cycle with food and water available *ad libitum*. All animal procedures were conducted according to the Scientific Procedures Act of 1986. No differences between +/+ and +/*stg* mice have been noted (Qiao et al., 1998; Hashimoto et al., 1999); therefore, we routinely combine +/+ and +/*stg* material for control experiments.

**Ligand autoradiography.** Assays were performed according to Korpi et al. (2002) with minor modifications. Briefly, mice were anesthetized with a lethal dose of pentobarbitone before transcardial perfusion with ice-cold PBS–NaNO<sub>2</sub> (0.1% w/v) for 3 min at 10 ml/min, followed by ice-cold PBS–sucrose (10% w/v) for 10 min at 10 ml/min. Brains were dissected and immediately frozen in isopentane (–40°C), 1 min before sectioning (14  $\mu$ m) at –21°C, and thaw mounting on polysine-coated glass slides (VWR International, Luttermworth, Leics, UK). Sections were air dried overnight and stored at –20°C until required. [<sup>3</sup>H]muscimol-labeled sections were preincubated in assay buffer, 0.31 M Tris-acetate, pH 7.1, for 15–20 min, before incubation in [<sup>3</sup>H]muscimol (20 nM) for 1 h at 4°C. GABA (1 mM) was used to define nonspecific binding. [<sup>3</sup>H]Ro15-4513 (20 nM) and [<sup>3</sup>H]flunitrazepam (5 nM) labeled sections were preincubated in assay buffer, 50 mM Tris-HCl, 120 mM NaCl, pH

7.4, for 15 min. Flunitrazepam (10  $\mu$ M) was used to define the flunitrazepam-sensitive (BZ-SR) and the flunitrazepam-insensitive (BZ-ISR) subtypes. Ro15-1788 (10  $\mu$ M) was used to define nonspecific binding.

**Quantification of receptor autoradiographs.** Autoradiographs and calibration standards were scanned at 1200 dots per inch using a flatbed scanner. Grayscale intensities were estimated using NIH ImageJ software. Calibration curves were constructed for each ligand/exposure period using [<sup>3</sup>H] standards at 0.1–109.4 nCi/mg (Amersham Biosciences) so grayscale intensity could be transformed into absolute radioactivity. Five random subdomains of each dentate gyrus from a minimum of six comparable sections per mouse strain were used to yield an estimated mean intensity. Nonspecific binding values were subtracted from mean intensity values to resolve specific ligand binding. Statistical analysis was by Student's *t* test, and *p* < 0.05 was considered to be statistically significant.

**Primary cerebellar granule cell cultures.** Cerebellar granule cell cultures were prepared from 5- to 6-d-old (postnatal day 5/6) mouse neonates as described previously (Ives et al., 2002). Granule cells were cultured in DMEM containing 10% (v/v) fetal calf serum, glutamine (2 mM), and gentamycin (50  $\mu$ g/ml), supplemented at 24 h, when appropriate, with 20 mM KCl (“25K” media). Fluorodeoxyuridine (80  $\mu$ M) was added at 48 h to suppress the proliferation of non-neuronal cells. CGCs (7 d *in vitro*) were harvested in 0.5 ml/35 mm dish of solubilizing buffer (50 mM Tris, pH 6.8, 2% w/v SDS, and 2 mM EDTA) so that the expression levels of GABAR subunit proteins could be determined by immunoblotting.

**Immunohistochemistry.** Immunohistochemistry was essentially as described previously (Thompson et al., 2002). Adult (2–6 months) mice were perfusion fixed with 4% (w/v) paraformaldehyde. Free-floating sections (30  $\mu$ m) were immunohistochemically stained using the Vectastain ABC Elite kit with 3,3'-diaminobenzidine (0.5 mg/ml) and H<sub>2</sub>O<sub>2</sub> (0.02%, v/v) in 50 mM Tris-buffered saline, pH 7.1, as horseradish peroxidase substrate.

**Antigen retrieval.** When required, sections were incubated in 0.05 M sodium citrate, pH 8.6, for 30 min at room temperature and then heated to 90°C for 70 min as described previously (Peng et al., 2004). Sections were cooled to room temperature and washed in TBS before processing for immunohistochemistry.

**Immunoblotting.** SDS-PAGE was performed in 10% polyacrylamide mini-slab gels (Thompson et al., 1998). Proteins were transferred to nitrocellulose membrane and probed with primary antibody overnight at 4°C at the following concentrations: anti-TARP $\gamma 2$ , 1–4  $\mu$ g/ml; anti-TARP $\gamma 8$ , 0.5  $\mu$ g/ml; anti-GluR2, 0.4–0.8  $\mu$ g/ml; anti-NMDA NR1, 1  $\mu$ g/ml; anti-GABAR  $\alpha 4$ , 0.5  $\mu$ g/ml; anti-GABAR  $\beta 3$ , 0.5  $\mu$ g/ml; anti-GABAR  $\gamma 2$ , 0.5  $\mu$ g/ml; anti-GABAR  $\delta$ , 1  $\mu$ g/ml; and anti-gephyrin, 1:250. The enhanced chemiluminescence Western blotting system was used to detect immunoreactive species on Hyperfilm. Band intensities were quantified as described previously (Ives et al., 2002) using NIH ImageJ software.

**Immunoprecipitations.** For immunoprecipitation (IP) of TARP complexes, Triton X-100 (1% v/v) soluble protein in incubation buffer [10 mM HEPES, pH 7.1, 100 mM KCl, 2 mM MgCl<sub>2</sub>, 1 mM EGTA, and a protease mixture of pepstatin-A (1  $\mu$ g/ml), leupeptin (1  $\mu$ g/ml), aprotinin (1  $\mu$ g/ml), PMSF (1 mM), and benzamidin (2 mM)] was mixed with antibody (10  $\mu$ g), applied to washed protein-A beads, and incubated overnight at 4°C. After centrifugation at 14,000  $\times$  *g* for 1 min, the supernatant containing unbound proteins was removed (“unbound fraction”). The beads were washed three times with 1 ml of incubation buffer. To elute the precipitated proteins from the beads, 35  $\mu$ l of 2 $\times$  SDS-PAGE sample buffer containing DTT (20 mM) was applied, incubated at 95°C for 5 min, and then centrifuged at 14,000  $\times$  *g* for 1 min. The supernatant (“immunoprecipitated fraction”) was removed and used for immunoblotting. To analyze the unbound fraction, 100  $\mu$ l samples were chloroform/methanol precipitated and resuspended in 50  $\mu$ l of 2 $\times$  SDS-PAGE sample buffer containing DTT (20 mM).

For immunoprecipitation of GABARs from dentate gyri, four control and four stargazer dentate gyri were homogenized by sonication in solubilization buffer comprising Na-deoxycholate (0.5% w/v), 10 mM Tris-Cl, pH 8.5, 150 mM NaCl, and protease inhibitors. After incubation for 30

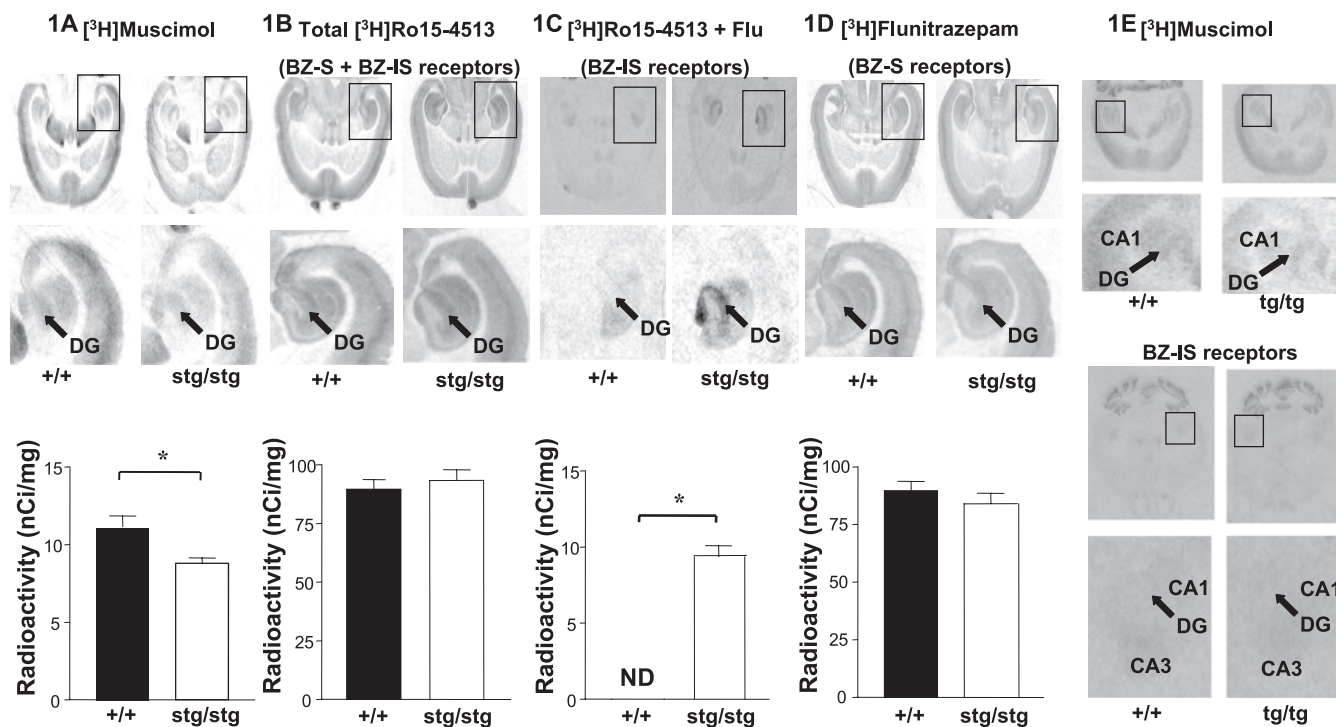


**Figure 1.** Distribution and abundance of GABA receptor subtypes expressed in the hippocampal formation of stargazer and tottering mice: *in situ* autoradiography. +/+, *stg*, and *tg* sections were incubated with [<sup>3</sup>H]muscimol (20 nM) to highlight  $\alpha 4\beta\delta$  GABA<sub>A</sub> receptors (A, E), [<sup>3</sup>H]Ro15-4513 (20 nM) to define BZ-S plus BZ-ISRs (B), [<sup>3</sup>H]Ro15-4513 (20 nM) plus flunitrazepam (Flu; 10  $\mu$ M) to define BZ-ISRs ( $\alpha 4\beta\gamma 2$ ) alone (C, E), and [<sup>3</sup>H]flunitrazepam (5 nM) to highlight BZ-SRs alone (D). Autoradiographs were quantified by grayscale densitometry using NIH ImageJ software. Five random subdomains of each dentate gyrus from a minimum of six comparable sections per mouse strain were used to yield an estimated mean intensity. In C, ND indicates that a signal above film background was not detected in the DG. In all cases, nonspecific binding was at the level of film background. \* indicates that values are statistically significantly different at the  $p < 0.05$  level.

min at room temperature and then 1 h at 4°C, the soluble material was isolated by centrifugation at 150,000  $\times$  g for 45 min. Soluble extract (70  $\mu$ g of protein) was incubated with 15  $\mu$ g of anti-GABA<sub>A</sub>  $\gamma 2$ (319–366) antibody overnight at 4°C. Immunoprecipitation (20  $\mu$ l) in IP-low buffer (50  $\mu$ l) [containing 50 mM Tris-Cl, pH 8.0, 150 mM NaCl, 1 mM EDTA, and Triton X-100 (0.2% v/v), supplemented with 5% (w/v) dry-milk powder] was subsequently added and incubated for 2 h at 4°C. Precipitate was pelleted by centrifugation at 2700  $\times$  g for 5 min, and the pellet was washed three times with 500  $\mu$ l of IP-low buffer before being resuspended in 70  $\mu$ l of SDS-PAGE sample buffer (NuPage Western blotting system; Invitrogen, Carlsbad, CA). Samples were subjected to SDS-PAGE, and Western blots were probed with digoxigenin-anti- $\gamma 2$ (319–366), anti- $\beta 3$ (345–408), and anti- $\alpha 4$ (1–14) antibodies. Primary antibodies were detected with anti-digoxigenin-alkaline phosphatase Fab fragments (Roche Diagnostics, Mannheim, Germany) and CDP-Star (Tropix, Bedford, MA). Immunoreactive species were visualized by chemiluminescence using the Bio-Rad (Hercules, CA) Fluor-S Multiimager and were quantified using Quantity One (Bio-Rad).

**Characterizing anti-TARP antibodies.** Full-length TARP $\gamma 2$ , TARP $\gamma 3$ , TARP $\gamma 4$ , and TARP $\gamma 8$  cDNAs subcloned into the mammalian expression vector pcDNA3 were a kind gift from Dr. Dane Chetkovich (Northwestern University, Chicago, IL). Plasmids were transiently transfected into HEK293 cells using Lipofectamine 2000 (Invitrogen, Paisley, UK) according to the instructions of the manufacturer. Cells were collected in solubilizing buffer [2% (w/v) SDS, 50 mM Tris, pH 6.8, and 2 mM EDTA] 48 h after transfection. These recombinantly expressed TARP isoforms were used to test the specificity of our anti-TARP antibodies in immunoblots.

**Electrophysiology.** Six- to 8-week-old male mice were anesthetized with pentobarbital (120 mg/kg, i.p.), and decapitated. Brains were rapidly dissected out into ice-cold modified artificial CSF (CSF) of the following composition (in mM): 248 sucrose, 3 KCl, 2 MgCl<sub>2</sub>, 1 CaCl<sub>2</sub>, 1.25 NaH<sub>2</sub>PO<sub>4</sub>, 26 NaHCO<sub>3</sub>, and 10 glucose (saturated with 95% O<sub>2</sub>, 5% CO<sub>2</sub>). Coronal slices, 300  $\mu$ m thick, were cut using a vibratome (VT1000S; Leica, Ora, Italy) and placed in a holding chamber at room

temperature (20–24°C) in aCSF of the following composition (in mM): 124 NaCl, 3 KCl, 1 MgCl<sub>2</sub>, 2 CaCl<sub>2</sub>, 1.25 NaH<sub>2</sub>PO<sub>4</sub>, 26 NaHCO<sub>3</sub>, and 10 glucose (bubbled with 95% O<sub>2</sub>, 5% CO<sub>2</sub>). Slices were incubated under these conditions for at least 1 h before recording began. Slices were placed in a custom-made recording chamber on the stage of a differential interference contrast microscope (E600FM DIC; Nikon, Tokyo, Japan) and perfused with room temperature (20–24°C) aCSF containing 2 mM kynurenic acid (Sigma, Castle Hill, New South Wales, Australia) at  $\sim$ 2 ml/min. Visually identified dentate granule cells were patched with thin-walled borosilicate electrodes (4–6 M $\Omega$ ) filled with the following solution (in mM): 125 CsCl, 10 HEPES, 10 EGTA, 5 QX-314 [2-(triethylamino)-N-(2,6-dimethylphenyl) acetamide], 1 Na<sub>2</sub>ATP, 0.3 LiGTP, pH 7.35 with CsOH (held at  $-70$  mV). Input conductance was measured using a 200 ms, 10 mV depolarizing step. Cells were held for at least 10 min to allow the pipette solution to dialyze the cell and the series resistance to equilibrate. If the series resistance increased above 30 M $\Omega$  or changed by  $>10\%$  during the course of a recording, the data from that cell were excluded from additional analysis. Miniature IPSCs (mIPSCs) were filtered at 3 kHz and logged at 10 kHz (micro 1401; Cambridge Electronics Design, Cambridge, UK) to Spike 4 software. Events were detected off-line with MiniAnalysis (Synaptosoft, Decatur, GA) with threshold criteria of 10 pA and 50 pA/ms. For kinetic analysis, only fast-rising (10–90% rise time  $<4$  ms) events ( $>100$  per cell) with an approximately exponential decay profile were included. We used two-tailed, paired, and unpaired *t* tests for hypothesis testing, and  $p < 0.05$  was regarded as significant.

## Results

### GABA<sub>A</sub> subtype expression in the dentate of stargazer

We initially investigated whether the stargazer mutation affected the distribution and abundance of the major GABA<sub>A</sub> subtypes expressed in the dentate gyrus. The distribution of [<sup>3</sup>H]muscimol binding in the DG of *stg* was mostly comparable with that in +/+ mice (Fig. 1A). The level of expression in the DG, however,

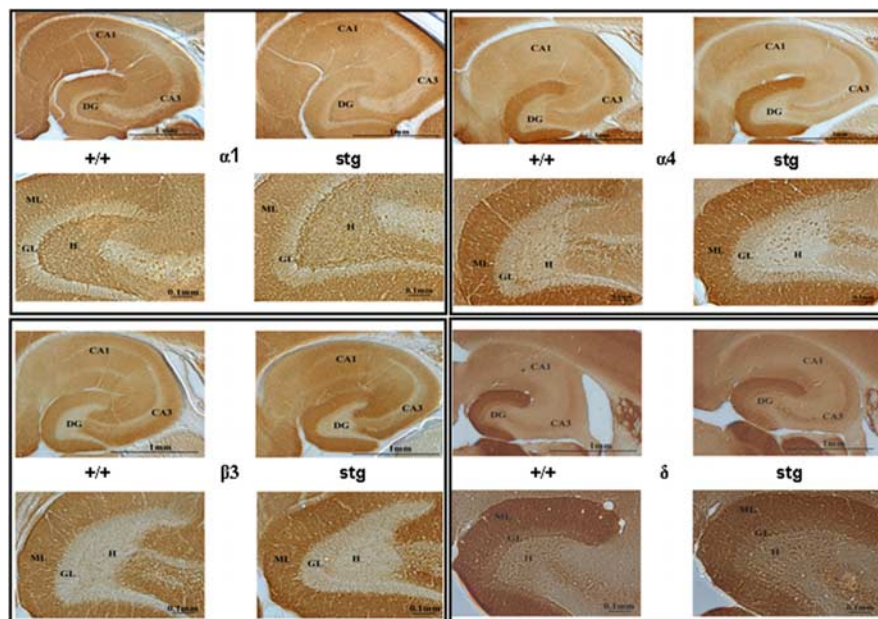


**Figure 2.** Immunohistochemical mapping of GABA $\alpha$ 1,  $\alpha$ 4,  $\beta$ 3, and  $\delta$  subunits in +/+ and *stg*. Paraformaldehyde-fixed adult +/+ and *stg* sections were immunostained with anti-GABA $\alpha$ 1 (0.25  $\mu$ g/ml),  $\alpha$ 4 (0.5  $\mu$ g/ml),  $\beta$ 3 (0.5  $\mu$ g/ml), and  $\delta$  (0.25  $\mu$ g/ml) subunit-specific antibodies. Although the relative distribution of GABA $\alpha$ 1,  $\alpha$ 4,  $\beta$ 3, and  $\delta$  subunits were essentially unaffected by the stargazer mutation, the relative intensity of GABA $\alpha$ 4 and  $\beta$ 3 subunit immunostaining was increased in the molecular layers of the dentate gyrus of *stg* compared with +/+.

was significantly reduced by  $21 \pm 8\%$  ( $p < 0.05$ ;  $n = 30$ ) relative to controls (Fig. 1A). Sections were probed with [ $^3$ H]Ro15-4513 to analyze the spatial expression pattern and relative propensity of the total repertoire of  $\gamma$ -subunit containing GABA $\alpha$ s in the DG. No significant difference was observed in either terms of distribution or comparative abundance (Fig. 1B) ( $p = 0.57$ ;  $n = 30$ ). Intriguingly, the subtype of [ $^3$ H]Ro15-4513 binding sites that are insensitive to flunitrazepam displacement (BZ-ISR) were strongly upregulated in *stg* DG (Fig. 1C) ( $p < 0.01$ ;  $n = 25$ ). This subtype of GABA $\alpha$  was undetectable in this brain region of adult control mouse (Fig. 1C, +/+). The spatial expression pattern and relative abundance of the flunitrazepam-sensitive subtype of GABA $\alpha$ s (BZ-SR) was qualitatively demonstrated in autoradiograms of +/+ and *stg* sections probed with [ $^3$ H]flunitrazepam (5 nM). No overt differences in distribution of [ $^3$ H]flunitrazepam labeling (Fig. 1D) or in the grayscale intensity of labeling (data not shown) were found. Because the grayscale intensities obtained with [ $^3$ H]flunitrazepam were beyond the highest calibration standard available to us and thus not suitable for quantification, we quantified the relative abundance of BZ-SRs by subtracting values obtained for BZ-ISR (Fig. 1C) from total [ $^3$ H]Ro15-4513 binding (BZ-SR plus BZ-ISR) (Fig. 1B). The level of expression of BZ-SR calculated by this route was not significantly different (Fig. 1D bottom) ( $p = 0.39$ ;  $n = 30$ ).

### Is GABA $\alpha$ subtype plasticity in the DG common to all absence epilepsy models?

To establish whether this switch in GABA $\alpha$  expression profile was unique to *stg* or possibly a common feature of absence epilepsy models, we performed GABA $\alpha$  ligand *in situ* autoradiography in another well studied mouse model of absence epilepsy, tottering (*tg*). We found no evidence of a decrease of high-affinity [ $^3$ H]muscimol binding sites or upregulation of BZ-ISR in *tg* DG (Fig. 1E).

### Evaluating GABA $\alpha$ subunit changes in the DG of stargazer

We next investigated whether the changes in GABA $\alpha$  subtype expression were paralleled by changes in the distribution (immunohistochemistry, hippocampal sections) and/or abundance (quantitative immunoblotting, DG membranes) of the principal GABA $\alpha$  subunits ( $\alpha$ 1,  $\alpha$ 2,  $\alpha$ 4,  $\beta$ 1,  $\beta$ 2,  $\beta$ 3,  $\gamma$ 2, and  $\delta$ ) expected to be expressed in the DG (Sperk et al., 1997) of age- and gender-matched +/+ and *stg* mice. No overt changes in the cellular distribution were observed ( $\alpha$ 1,  $\alpha$ 4,  $\beta$ 3, and  $\delta$  are shown in Fig. 2), although the intensity of staining (expression) for GABA $\alpha$ 4 and  $\beta$ 3 subunits was higher in the entire molecular layer of the DG of *stg* mice relative to +/+ (Fig. 2). GABA $\alpha$   $\delta$  subunit expression, in contrast, was downregulated in the entire molecular layer of the DG of *stg* mice relative to +/+ (Fig. 2), although this observation was variable and not seen in all sections from all mice studied. No consistent changes in the intensity of staining with GABA $\alpha$ 1,  $\alpha$ 2,  $\beta$ 1,  $\beta$ 2, and  $\gamma$ 2 specific antibodies were observed (Fig. 2). Quantitative immunoblotting identified GABA $\alpha$ 4 and  $\beta$ 3 subunits as

the only proteins studied that were significantly changed, being upregulated after normalization to  $\beta$ -actin expression by  $37 \pm 12\%$  ( $n = 7$ ;  $p = 0.0003$ ) and  $39 \pm 28\%$  ( $n = 6$ ;  $p = 0.026$ ), respectively, relative to controls (Fig. 3A). Expression levels of GABA $\alpha$   $\delta$  and  $\gamma$ 2, NMDA receptor NR1, AMPA receptor GluR2, and GABA $\alpha$  anchoring protein gephyrin were not significantly different.

We asked whether the changes in GABA $\alpha$  subunit expression in DG granule cells might be an adaptive response to SWDs pervading the hippocampal formation of *stg*. We subjected cultured CGCs from +/+ mice to KCl-mediated depolarization to mimic a chronically depolarizing, seizure-like scenario *in vitro*. The GABA $\alpha$   $\alpha$ 4 subunit is not normally detected in CGCs, but, after KCl-mediated depolarization,  $\alpha$ 4 expression was clearly switched on (Fig. 3B). A concomitant upregulation of the  $\beta$ 3 subunit was also detected (Fig. 3B), whereas expression of GABA $\alpha$   $\gamma$ 2 was unaffected, supporting our *in vivo* data that upregulation of  $\alpha$ 4 and  $\beta$ 3 subunits in DG granule cells of *stg* occur in response to inputs from hyperexcitable afferents.

To verify that the upregulation of BZ-ISR in the *stg* DG was a consequence of increased expression of  $\alpha$ 4 $\beta$ 3 $\gamma$ 2 receptors, we dissected out dentate gyri from +/+ and *stg*. Na-deoxycholate-solubilized extracts were subsequently immunoprecipitated using anti-GABA $\alpha$   $\gamma$ 2 antibodies to isolate GABA $\alpha$   $\gamma$ 2-containing receptors. As expected,  $\alpha$ 4 was barely detectable in the  $\gamma$ 2-containing subpopulation of receptors from +/+ DG, although it was clearly detectable in *stg* DG (experiments not shown). Changes in coassociation of  $\gamma$ 2 with  $\alpha$ 4 and  $\beta$ 3 subunits were then quantified by comparing the protein staining of the respective subunits in  $\gamma$ 2-containing receptors of +/+ and *stg* DG. As indicated in Table 1, protein staining for  $\gamma$ 2 subunits was comparable in  $\gamma$ 2 precipitates of +/+ and *stg*, reflecting a similar amount of  $\gamma$ 2-containing receptors in DG of these mice (Fig. 3). The amounts of  $\alpha$ 4 subunits, however, were dramatically higher

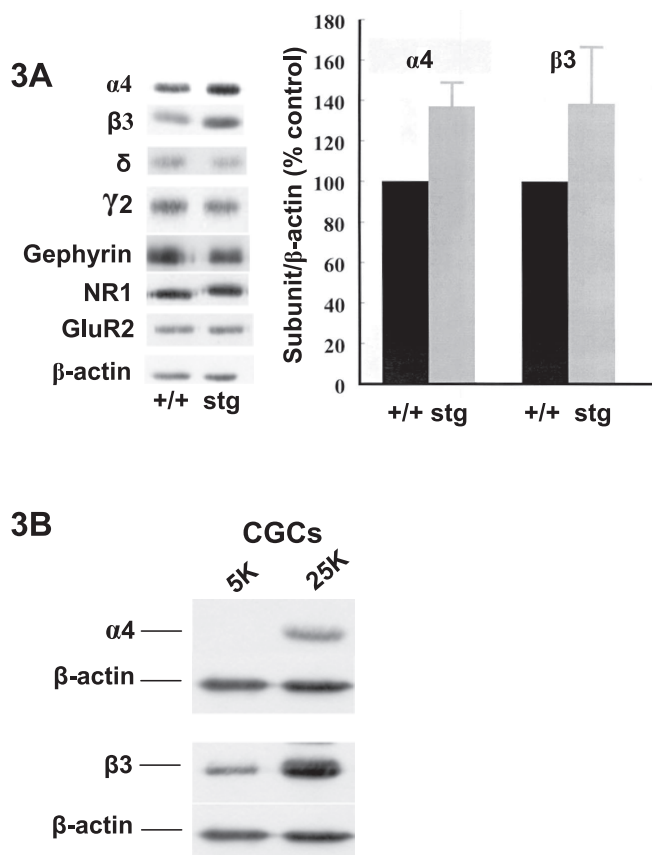


**Figure 3.** GABAR  $\alpha 4$  and  $\beta 3$  subunit levels are selectively upregulated in the DG of *stg* mice *in vivo* and in chronically depolarized cerebellar granule cells *in vitro*. **A**, Dentate gyri membranes from adult *+/+* and *stg* mice were analyzed by quantitative immunoblotting (minimum of 4 mice of each strain and 2 immunoblots per mouse). Representative lanes of equal protein loading for each strain are shown for comparison. Only GABAR  $\alpha 4$  and  $\beta 3$  subunit levels were significantly ( $p < 0.05$ ) affected by the mutation, being increased relative to controls by  $37 \pm 12\%$  ( $n = 7$ ;  $p = 0.0003$ ) and  $39 \pm 28\%$  ( $n = 6$ ;  $p = 0.026$ ), respectively. **B**, Cerebellar granule cells were cultured under basal, “polarized” conditions (5 mM KCl) and “depolarized” conditions (25 mM KCl), the latter to mimic chronically depolarizing seizure activity. Cells were collected at 7 d *in vitro* and analyzed by immunoblotting. As in *stg* dentate granule cells, GABAR  $\alpha 4$  and  $\beta 3$  subunits were upregulated.

(by 95%) in  $\gamma 2$  precipitates from *stg* than from *+/+*, confirming upregulation of assembled  $\alpha 4\gamma 2$ -containing receptors in *stg*. Likewise, coassociation of  $\beta 3$  with  $\gamma 2$  was also upregulated (by ~24%) in *stg* DG compared with *+/+* (Table 1).

#### Do the GABAR subunit changes result in modifications to synaptic GABA function?

There was no significant difference in the input conductance of DG granule cells from stargazer and their nonepileptic littermates ( $0.99 \pm 0.13$  vs  $1.29 \pm 0.23$  nS;  $n = 4$ ;  $p > 0.05$ , unpaired *t* test). Bicuculline methiodide (BMI) (100  $\mu$ M) sensitive GABAR-mediated tonic currents were significantly lower in the dentate granule cells of epileptic *stg* mice compared with asymptomatic littermates ( $7.5 \pm 0.2$  vs  $3.5 \pm 0.7$  pA;  $n = 4$ –5;  $p < 0.05$ , unpaired *t* test) (Fig. 4). BMI significantly reduced the total input conductance in both phenotypes (*+/+*,  $0.99 \pm 0.13$  vs  $0.71 \pm 0.19$  nS,  $n = 4$ ,  $p < 0.05$ , paired *t* test; *Stg*,  $1.29 \pm 0.23$  vs  $0.98 \pm 0.21$  nS,  $n = 4$ ,  $p < 0.05$ , paired *t* test). However, the mean decrease in input conductance as a percentage of the initial conductance was larger in *+/+* than in *stg* mice, although this difference did not reach statistical significance ( $32.4 \pm 10.8$  vs  $21.1 \pm$

**Table 1.** Western blot analysis of the relative abundance of  $\alpha 4$  and  $\beta 3$  subunits coassociated with  $\gamma 2$  subunits in the dentate gyrus of control (*+/+*) and stargazer (*stg*) mice

Subunits detected	Control		Stargazer	
	% of mean	Mean %	% of mean (controls)	Mean %
$\gamma 2$	102	100	110	103
	98		96	
$\alpha 4$	88	100	189	195
	112		200	
$\beta 3$	104	100	117	124
	96		130	

Dentate gyri from four *+/+* and four *stg* mice were extracted with deoxycholate buffer. Equivalent amounts of extracted protein from each mouse strain was incubated with  $\gamma 2(319$ –366) antibodies. Precipitated proteins were subjected to immunoblotting using digoxigenized  $\gamma 2(319$ –366),  $\alpha 4(1$ –14), and  $\beta 3(345$ –408) antibodies as probes. Immunoreactive proteins were identified by chemiluminescence, and intensity of protein staining was quantified using the Bio-Rad Fluor-S Multi-Imager. Data are from a single experiment performed in duplicate. Results are expressed as a percentage of the mean value of staining of the respective subunit determined for  $\gamma 2$ -precipitated *+/+* extracts. The data indicated that comparable amounts of  $\gamma 2$ -containing receptors were precipitated from *+/+* and *stg* tissue extracts. In receptors precipitated from *stg*, however, significantly greater amounts of  $\alpha 4$  and  $\beta 3$  subunits were associated with  $\gamma 2$ -containing receptors than from *+/+*.

7.7%;  $n = 4$ ;  $p > 0.05$ , unpaired *t* test) (Fig. 4D). The amount of tonic current was enhanced by the  $\delta$  selective neurosteroid tetrahydrodeoxycorticosterone (THDOC) (100 nM) (Stell et al., 2003), but the amount of tonic current was still significantly lower in *stg* mice in the presence of the positive allosteric modulator ( $19.8 \pm 1.0$  vs  $11.1 \pm 2.6$  pA;  $n = 4$ –5;  $p < 0.05$ , unpaired *t* test) (Fig. 4). Because spillover from synaptic activity is the likely source of the GABA that activates extrasynaptic GABARs, the difference in GABAR-mediated tonic current could reflect a difference in phasic GABA release, but there was no significant difference in the rate ( $0.92 \pm 0.17$  Hz for *+/+* vs  $0.93 \pm 0.14$  Hz for *stg*;  $n = 6$ ;  $p > 0.05$ , unpaired *t* test) or amplitude ( $50.1 \pm 4.6$  pA for *+/+* vs  $48.3 \pm 2.2$  pA for *stg*;  $n = 6$ ;  $p > 0.05$ , unpaired *t* test) of spontaneous IPSCs (data not shown). We postulated that the alteration in GABAR subunit composition reported here may result in alterations in the kinetics of phasic inhibitory currents. mIPSCs were isolated with tetrodotoxin (500 nM), and the kinetics of these events were compared between *+/+* and *stg* mice. Averaged mIPSCs were essentially identical in epileptic and non-epileptic animals, and there was no significant difference in area ( $0.435 \pm 0.04$  nA/ms for *+/+* vs  $0.43 \pm 0.04$  nA/ms for *stg*;  $n = 4$ ;  $p > 0.05$ , unpaired *t* test) (Fig. 5) or amplitude ( $44.5 \pm 2.2$  pA for *+/+* vs  $44.8 \pm 4.8$  pA for *stg*;  $n = 4$ ;  $p > 0.05$ , unpaired *t* test) (Fig. 5).

#### Are the GABAR rearrangements in the DG caused by the loss of TARP $\gamma 2$ in this brain region?

To test whether the GABAR rearrangements we observed were a direct consequence of the stargazer mutation, we used peptide affinity-purified rabbit anti-TARP antibodies to elucidate the distribution and abundance of TARP isoforms expressed in the DG. A panel of our affinity-purified rabbit anti-peptide polyclonal antibodies to the C-terminus sequence of TARP $\gamma 2$  was found to cross-react with TARP $\gamma 3$  and TARP $\gamma 8$  when screened against recombinantly expressed TARP isoforms (data not shown). We initially used this pan-TARP antibody as a probe in immunoblots against whole forebrain membranes from *+/+* and *stg* mice. Three prominent immunoreactive species were recognized in this tissue from *+/+*, with  $M_r$  values of ~55, ~48, and 36–41 kDa (Fig. 6A). The 36–41 kDa species exhibits the same apparent molecular mass as recombinant TARP $\gamma 2$  and was absent in *stg* (essentially TARP $\gamma 2^{-/-}$  tissue), suggesting that the 36–41 kDa species corresponds to TARP $\gamma 2$ . The ~55 and ~48 kDa bands likely represent other TARP isoforms that this anti-

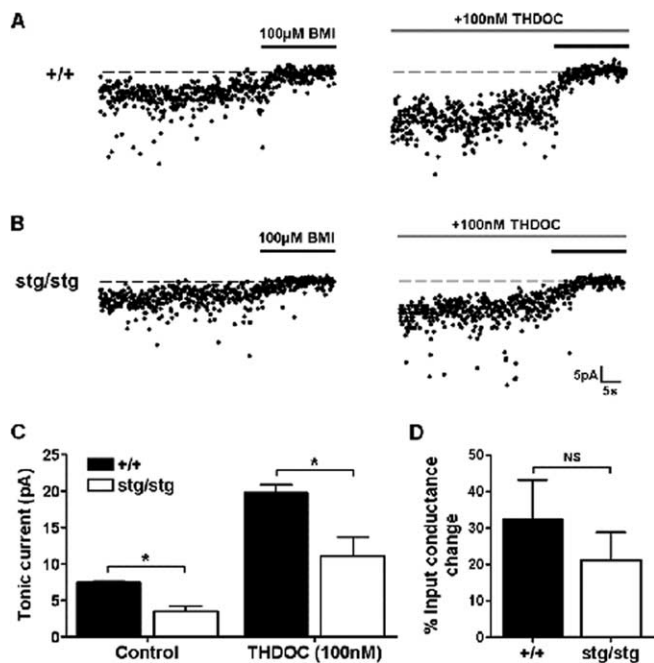


**Figure 4.** Tonic GABA-mediated current in dentate gyrus granule cells. **A**, Representative traces of tonic GABA-mediated currents in granule cells from +/+ mice and the effect of the  $\delta$  subunit-selective neurosteroid THDOC (100 nM). Tonic currents were defined by the shift to current baseline after application of GABA antagonist BMI (100  $\mu$ M). **B**, Representative traces of tonic GABA-mediated currents in granule cells from *stg* mice and the effect of the  $\delta$  subunit-selective neurosteroid THDOC (100 nM). **C**, Cells from +/+ mice showed significantly more tonic current than those from *stg* mice ( $7.5 \pm 0.2$  vs  $3.5 \pm 0.7$  pA;  $n = 4$ – $5$ ;  $p < 0.0017$ , unpaired  $t$  test). In the presence of THDOC (100 nM), the tonic current was enhanced, and cells from +/+ mice showed significantly more tonic current than those from *stg* mice ( $19.8 \pm 1.0$  vs  $11.1 \pm 2.6$  pA;  $n = 4$ – $5$ ;  $p < 0.0245$ , unpaired  $t$  test). The solid black line indicates application of BMI (100  $\mu$ M) to define tonic current. **D**, The decrease in input conductance caused by BMI was not significantly (NS) different between +/+ and *stg* mice ( $32.4 \pm 10.8$  vs  $21.1 \pm 7.7$ %;  $n = 4$ ;  $p > 0.05$ , unpaired  $t$  test). \* indicates that values are statistically significantly different at the  $p < 0.05$  level.

body recognizes, e.g., TARP $\gamma$ 8, that has a comparable mass when expressed in heterologous cells (data not shown). Interestingly, these bands appear less intense in whole forebrain from *stg* than from +/+. When we used this antibody as a probe for immunohistochemical mapping of TARP isoform distribution, we observed less intense immunostaining in the DG of *stg* relative to +/+ (Fig. 6B). The reduction in the immunostaining was consistent with the ablated expression of TARP $\gamma$ 2 in *stg* DG, because the *stg* mice are essentially TARP $\gamma$ 2<sup>-/-</sup> mutants. However, when we used dentate gyri from +/+ and *stg* for immunoblotting, we surprisingly found that the 36–41 kDa TARP $\gamma$ 2 protein, present in whole forebrain membranes derived from +/+ and absent from *stg* mice (Fig. 6A), was undetectable in the DG from +/+ mice. Only the  $M_r \sim 55$  kDa immunoreactive species was detected in the DG (Fig. 6A). This corresponded in mass to TARP $\gamma$ 8, a TARP-isoform known to be almost exclusively expressed in the hippocampal formation (Bredt and Nicoll, 2003). We subsequently raised a TARP $\gamma$ 8-specific antibody and verified that the  $M_r \sim 55$  kDa species identified by the pan-TARP antibody was TARP $\gamma$ 8 and that its expression was reduced in *stg* DG. By quantitative immunoblotting, we estimated that the expression of this protein was reduced by  $33 \pm 1\%$  in *stg* DG membranes relative to +/+, in accordance with the reduced intensity of staining observed in the *stg* DG *in situ* (Fig. 6B). To verify that TARP $\gamma$ 8 was indeed an AMPAR-associated protein, we subjected Triton

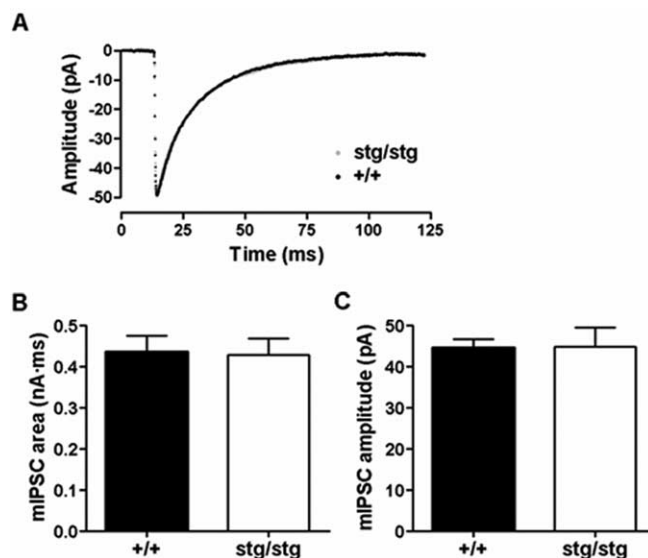


**Figure 5.** Kinetic features of mIPSCs in dentate granule cells. **A**, Averaged mIPSCs recorded in granule cells from *stg* and +/+ were essentially superimposable ( $n = 4$ ). **B**, The mean area of mIPSCs from granule cells from +/+ mice and *stg* was not significantly different ( $0.435 \pm 0.039$  nA·ms for +/+ vs  $0.429 \pm 0.039$  nA·ms for *stg*;  $n = 4$ ;  $p > 0.05$ ). **C**, The mean amplitude of mIPSCs in granule cells from +/+ mice and *stg* was not significantly different ( $44.5 \pm 2.2$  pA for +/+ vs  $44.8 \pm 4.8$  pA for *stg*;  $n = 4$ ;  $p > 0.05$ ).

X-100-soluble DG from +/+ mice to an immunoprecipitation assay using the pan-TARP antibody. Because in the DG this antibody only labels TARP $\gamma$ 8 (Fig. 6A), it could be used to see whether this protein is associated with AMPAR. AMPAR GluR2 was coprecipitated, verifying that the protein recognized by this antibody was an AMPAR-associated protein (Fig. 6C). This was further verified by performing the same immunoprecipitation assay but using our anti-TARP $\gamma$ 8-specific antibody. GluR2 was likewise coprecipitated (data not shown).

## Discussion

The *stg* mutation selectively and completely ablates expression of TARP $\gamma$ 2 (Ives et al., 2004), a member of the TARP family of AMPAR synaptic targeting and/or trafficking proteins (Chen et al., 2000; Tomita et al., 2003; Rouach et al., 2005). The effects of this mutation, however, on the hippocampal formation and cerebellum appear to be diametrically opposed. In the latter case, mossy fiber–CGC synapses are predictably silent, and the CGCs are functionally deafferented and fail to express BDNF (Qiao et al., 1998; Hashimoto et al., 1999). Paradoxically, the hippocampus experiences spontaneous bursting activity and intermittent elevations of BDNF (Qiao and Noebels, 1993b; Chafetz et al., 1995; Nahm and Noebels, 1998).

## GABA<sub>A</sub> plasticity

Inhibitory GABAergic networks adapt to changes in the strength of their excitatory inputs (Nusser et al., 1998; Ives et al., 2002; Leroy et al., 2004; Peng et al., 2004; Suzuki et al., 2005) and any accompanying changes in BDNF/TrkB signaling (Yamada et al., 2002; Elmariah et al., 2004; Jovanovic et al., 2004; Sato et al., 2005). In electrically silent, BDNF-deficient CGCs of *stg*, GABA<sub>A</sub> receptor  $\alpha$ 6 (the cerebellar counterpart of the  $\alpha$ 4 subunit in the DG) and  $\beta$ 3 subunits and BZ-IS receptors were downregulated, whereas flunitrazepam-sensitive (BZ-S) receptors were unaffected (Thompson et al., 1998). In electrically hyperexcitable, BDNF overexpressing dentate granule cells of *stg*, we predicted

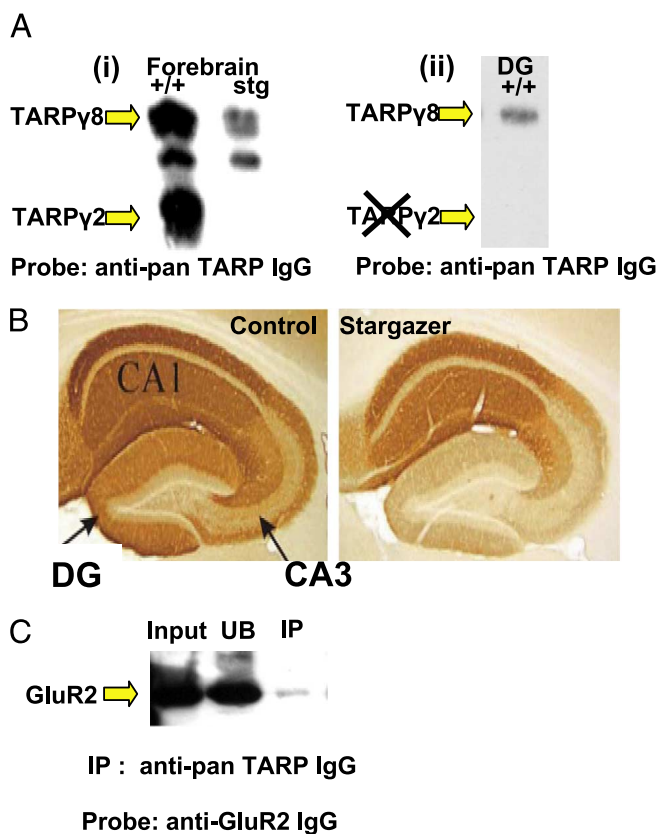


**Figure 6.** Characterizing TARP expression in the dentate gyrus. **Ai**,  $+/+$  and  $stg$  forebrain membranes were probed with our anti-pan-TARP antibody. Three prominent immunoreactive species were identified, with  $M_r$  values of  $\sim 55$ ,  $\sim 48$ , and  $36-41$  kDa; only the  $36-41$  kDa TARP $\gamma$ 2 protein is totally absent from  $stg$ . The  $\sim 55$  and  $\sim 48$  kDa species possibly represent TARP isoforms and are clearly less prominent in  $stg$  versus  $+/+$ , despite equal protein loading per lane. **Aii**, TARP $\gamma$ 2 is undetectable in the DG of  $+/+$ , and only the  $M_r \sim 55$  kDa protein is detected. This immunopositive species was also recognized by the TARP $\gamma$ 8-specific antibody in  $+/+$  and  $stg$  DG, identifying it as TARP $\gamma$ 8. **B**, Paraformaldehyde-fixed sections from  $+/+$  and  $stg$  mice were immunohistochemically probed with our anti-pan-TARP antibody. The DG in  $+/+$  was clearly more heavily stained than the corresponding area in  $stg$ . **C**, TARP $\gamma$ 8 and its associated interacting proteins were immunoprecipitated from Triton X-100 (1% v/v) soluble extracts of DG from  $+/+$  mice using the anti-pan-TARP antibody. Input ( $+/+$  DG) is Triton X-100-soluble extract of DG from  $+/+$  mice. UB is material that remained in the soluble supernatant after the immunoprecipitation. IP is immunoprecipitated material. These samples were probed with anti-GluR2 antibody to screen for the presence of interacting AMPAR. The GluR2 signal in the input lane represents 35% of material used in the IP.

opposite effects, which indeed we found. Steady-state levels of GABA<sub>A</sub>  $\alpha$ 4 and  $\beta$ 3 and BZ-IS [ $^3$ H]Ro15-4513 binding sites, a pharmacological fingerprint of  $\alpha$ 4 $\beta$ 2 subunit-containing GABA<sub>A</sub> receptors in the forebrain (Mihalek et al., 1999; Sun et al., 2004), were upregulated in the DG of  $stg$  (Figs. 1C, 3). Expression of the BZ-S subtype of GABA<sub>A</sub> receptors was not significantly affected, emphasizing the specificity of the receptor switch we observed.

In the DG of wild-type mice,  $\alpha$ 4 preferentially assembles with  $\delta$  to form  $\alpha$ 4 $\beta$  $\delta$  receptors. There is little evidence for its assembly into  $\alpha$ 4 $\beta$  $\gamma$ 2 receptors unless the ability to assemble with  $\delta$  is compromised, e.g., in GABA<sub>A</sub>  $\delta^{-/-}$  (Mihalek et al., 1999; Korpi et al., 2002; Sun et al., 2004). In  $stg$ , we propose that the assembly of  $\alpha$ 4-containing receptors is compromised. By *in situ* autoradiography, high-affinity [ $^3$ H]muscimol binding selectively highlights  $\alpha$ 4 $\beta$  $\delta$  GABA<sub>A</sub> receptors in the forebrain (Mihalek et al., 1999; Korpi et al., 2002), which constituted a smaller proportion of total  $\alpha$ 4-containing receptors in  $stg$  compared with  $+/+$ . The  $\alpha$ 4 $\beta$  $\gamma$ 2 subtype (BZ-ISRs) however, was a prominent GABA<sub>A</sub> subtype in the

DG of  $stg$ , constituting  $\sim 10\%$  of total [ $^3$ H]Ro15-4513 binding sites, although it was undetectable in  $+/+$  (Fig. 1C). Thus, our data imply that  $\alpha$ 4 $\beta$  $\gamma$ 2 receptors arose in  $stg$  DG at the expense of  $\alpha$ 4 $\beta$  $\delta$  receptors. This transformation in GABA<sub>A</sub> subtypes is entirely compatible with previous observations in both temporal lobe epilepsy (Nusser et al., 1998) and electroshock seizure models (Clark, 1998) and would predict a switch from tonic GABA responsive, neurosteroid-sensitive extrasynaptic  $\alpha$ 4-containing GABA<sub>A</sub> receptors ( $\alpha$ 4 $\beta$  $\delta$ ) to potentially synaptic  $\alpha$ 4-containing GABA<sub>A</sub> receptors that are relatively neurosteroid insensitive and respond in phasic mode to synaptically released GABA ( $\alpha$ 4 $\beta$  $\gamma$ 2) (Nusser and Mody, 2002), a mechanism consistent with the recent observations of Elmariah et al. (2004). Our electrophysiological data support this prediction, because DG granule cells in  $stg$  show a reduced amount of neurosteroid-sensitive tonic current compared with their nonepileptic littermates (Stell et al., 2003). Because of the low abundance of  $\alpha$ 4 $\beta$  $\gamma$ 2 receptors ( $<10\%$  of total receptors) and the lack of drugs selectively modulating these receptors (Sieghart and Ernst, 2005), their presence at the synapse and function could not be investigated.

Our immunohistochemical studies indicated that  $\delta$  expression was downregulated in  $stg$  DG (Fig. 2). A reduction in expression of the  $\delta$  subunit would have been entirely compatible with the reduction in *in situ* muscimol binding and with the emergence of BZ-ISRs in the  $stg$  DG. However, this difference in  $\delta$  immunostaining was variable between sections, a phenomenon that could not be explained by variability in the gender or age of animals used (our unpublished observation). Furthermore, the level of expression of  $\delta$  and  $\gamma$ 2 subunits were not significantly different in  $stg$  compared with controls when isolated dentate gyri were analyzed by immunoblotting (Fig. 3), nor did we see variability in our autoradiographic studies, in which all  $stg$  sections investigated showed evidence of the switch in GABA<sub>A</sub> subtypes. Studies in an appropriate dynamic cell system will be required to elucidate the mechanism that underpins the switch from  $\alpha$ 4 $\beta$  $\delta$  to  $\alpha$ 4 $\beta$  $\gamma$ 2 GABA<sub>A</sub> receptors. Interestingly, we found that chronically depolarizing cerebellar granule cells *in vitro* upregulates  $\alpha$ 4 and  $\beta$ 3 subunits in an L-type voltage-gated calcium channel-sensitive manner (H. L. Payne, J. H. Ives, W. Sieghart, and C. L. Thompson, unpublished observations). Calcineurin phosphatase activity downregulates GABA<sub>A</sub>  $\delta$  expression (Sato et al., 2005); thus, activity-dependent calcium signaling-mediated upregulation of GABA<sub>A</sub>  $\alpha$ 4 and  $\beta$ 3 and downregulation of  $\delta$  offers a tentative mechanistic framework for future studies to evaluate what dictates the balance between expression and assembly of extrasynaptic ( $\alpha$ 4 $\beta$  $\delta$  receptors) and synaptic ( $\alpha$ 4 $\beta$  $\gamma$ 2 receptors) GABA<sub>A</sub> receptors in the dentate granule cells.

One potential avenue for additional study is the influence of BDNF on GABA<sub>A</sub> receptor plasticity in  $stg$  because the contrasting effects on GABA<sub>A</sub> receptor expression in the DG and CGCs are mirrored by reciprocal effects on BDNF expression. BDNF/TrkB signaling has been implicated in the induction of both hyperexcitable mossy-fiber reentrant circuits in the DG (Koyama et al., 2004) and GABAergic plasticity. The latter included increased expression, surface trafficking and presumably stabilization of GABA<sub>A</sub>  $\beta$ 3 subunit-containing receptors (Yamada et al., 2002; Jovanovic et al., 2004), increased GABA<sub>A</sub> cluster number, and synaptic localization (Elmariah et al., 2004). These features are all consistent with those reported here in  $stg$ .

The GABA<sub>A</sub> rearrangements we report in  $stg$  DG are, however, not a landmark feature of absence epilepsy. The absence epileptic mouse model tottering experiences a frequency of burst activity in the hippocampal formation that is similar to that re-

ported in *stg* (~6 Hz), but the abnormal DG GABAR profile is not reciprocated (Fig. 1E). However, the rate and duration of burst activity in tottering is approximately half that recorded in *stg*, and mossy-fiber axon collateralization is less extensive, as is the severity of their epileptic phenotype (Qiao and Noebels, 1993a; Zhang et al., 2002), leading us to propose that a threshold of hyperexcitability needs to be surpassed to activate the mechanisms responsible for the GABAergic plasticity evident in *stg* mice. It has been proposed recently that GABAergic plasticity is a homeostatic neuronal response that aims to balance network excitability (Elmariah et al., 2004). This may explain why high-frequency SWDs entering the hippocampal formation illicit re-wiring similar to convulsant seizures but fail to induce the cell death that is a prominent feature of the latter.

### TARP expression in the dentate

To rationalize the contrasting effects of the stargazer mutation in the cerebellum and hippocampus, we proposed two possibilities. (1) If TARP $\gamma$ 2 is expressed in the DG, then it must selectively regulate the activity of inhibitory networks, thus, burst activity in the *stg* hippocampus. (2) Alternatively, the failure to express TARP $\gamma$ 2 in other brain regions in *stg* (Qiao and Noebels, 1993a) was responsible for increased excitatory drive entering the *stg* DG. Using our pan-TARP and TARP $\gamma$ 8-specific antibodies, we showed that TARP $\gamma$ 2 is not present in the DG of *+/+* mice. Our data provide compelling evidence that the dentate expresses the TARP $\gamma$ 8 isoform exclusively. Furthermore, TARP $\gamma$ 8 was downregulated in *stg* DG (Fig. 6C), consistent with the reduced immunostaining seen *in situ* (Fig. 6A), thus providing evidence that TARP $\gamma$ 8 expression is regulated by electrical activity. Because TARP $\gamma$ 2 is not expressed in DG, downregulation of TARP $\gamma$ 8, mossy-fiber axon collateralization, and receptor plasticity in the *stg* hippocampus (Chafetz et al., 1995; Nahm et al., 1998) has to arise through failed expression of TARP $\gamma$ 2 elsewhere in the stargazer brain. Despite the reduction of TARP $\gamma$ 8 expression in *stg* DG, we found no evidence of significant changes in the expression levels of AMPAR subunits (Fig. 3). This is in contrast to the TARP $\gamma$ 8<sup>-/-</sup> mouse, in which hippocampal GluR expression was found to be severely compromised (Rouach et al., 2005). We assume that the minor reduction of TARP $\gamma$ 8 expression in the *stg* DG is too small for us to detect any associated changes in the levels of AMPAR subunits.

In conclusion, we have shown that TARP $\gamma$ 2 is not expressed in the granule cells or interneurons of the dentate gyrus. The function of TARPs in the DG would appear to be the exclusive responsibility of the TARP $\gamma$ 8 isoform, which we show operates as an AMPAR-interacting protein (Fig. 6D). The inability of *stg* to express TARP $\gamma$ 2 results in expression of the GABAR  $\alpha$ 4 $\beta$ 3 $\gamma$ 2 subtype in the DG that would be predicted to confer unique GABAergic properties to the DG and impart the potential for relocalization of  $\alpha$ 4 $\beta$ 3 subunits to inhibitory synapses at the apparent expense of  $\delta$ -associated  $\alpha$ 4 $\beta$ 3 subunits in extrasynaptic domains. Whether these GABAR rearrangements are adaptive responses to high-frequency excitatory oscillations from DG afferents has yet to be fully resolved. Nonetheless, this provides an intriguing system with which to study mechanisms that dictate GABAR expression, assembly, and targeting.

### References

- Bredt DS, Nicoll RA (2003) AMPA receptor trafficking at excitatory synapses. *Neuron* 40:361–379.
- Chafetz RS, Nahm WK, Noebels JL (1995) Aberrant expression of neuropeptide Y in hippocampal mossy fibers in the absence of local cell injury following the onset of spike-wave synchronization. *Brain Res Mol Brain Res* 31:111–121.
- Chen L, Chetkovich DM, Petralia RS, Sweeney NT, Kawasaki Y, Wenthold RJ, Bredt DS, Nicoll RA (2000) Stargazin regulates synaptic targeting of AMPA receptors by two distinct mechanisms. *Nature* 408:936–943.
- Clark M (1998) Sensitivity of the rat hippocampal GABA<sub>A</sub> receptor  $\alpha$ 4 subunit to electroshock seizures. *Neurosci Lett* 250:17–20.
- Elmariah SB, Crumling MA, Parsons TD, Balice-Gordon RJ (2004) Postsynaptic TrkB-mediated signaling modulates excitatory and inhibitory neurotransmitter receptor clustering at hippocampal synapses. *J Neurosci* 24:2380–2393.
- Hashimoto K, Fukaya M, Qiao X, Sakimura K, Watanabe M, Kano M (1999) Impairment of AMPA receptor function in cerebellar granule cells of ataxic mutant mouse stargazer. *J Neurosci* 19:6027–6036.
- Ives JH, Drewery DL, Thompson CL (2002) Differential cell surface expression of GABA<sub>A</sub> receptor  $\alpha$ 1,  $\alpha$ 6,  $\beta$ 2 and  $\beta$ 3 subunits in cultured mouse cerebellar granule cells—influence of cAMP-activated signalling. *J Neurochem* 80:317–327.
- Ives JH, Fung S, Tiwari P, Payne HL, Thompson CL (2004) Microtubule associated protein light chain 2 is a stargazin-AMPA receptor complex interacting protein, *in vivo*. *J Biol Chem* 279:31002–31009.
- Jovanovic JN, Thomas P, Kittler JT, Smart TG, Moss SJ (2004) Brain-derived neurotrophic factor modulates fast synaptic inhibition by regulating GABA<sub>A</sub> receptor phosphorylation, activity, and cell-surface stability. *J Neurosci* 24:522–530.
- Korpi ER, Mihalek RM, Sinkkonen ST, Hauer B, Hevers W, Homanics GE, Sieghart W, Luddens H (2002) Altered receptor subtypes in the forebrain of GABA<sub>A</sub> receptor  $\delta$  subunit-deficient mice: recruitment of  $\gamma$ 2 subunits. *Neuroscience* 109:733–743.
- Koyama R, Yamada MK, Fujisawa S, Katoh-Semba R, Matsuki N, Ikegaya Y (2004) Brain-derived neurotrophic factor induces hyperexcitable reentrant circuits in the dentate gyrus. *J Neurosci* 24:7215–7224.
- Leroy C, Poisbeau P, Keller AF, Nehlig A (2004) Pharmacological plasticity of GABA<sub>A</sub> receptors at dentate gyrus synapses in a rat model of temporal lobe epilepsy. *J Physiol (Lond)* 557:473–487.
- Letts VA, Felix R, Biddlecome GH, Arikath J, Mahaffey CL, Valenzuela A, Bartlett II, FS, Mori Y, Campbell KP, Frankel WN (1998) The mouse stargazer gene encodes a neuronal Ca<sup>2+</sup>-channel  $\gamma$  subunit. *Nat Genet* 19:340–347.
- Mihalek RM, Banerjee PK, Korpi ER, Quinlan JJ, Firestone LL, Mi ZP, Lag- enauer C, Tretter V, Sieghart W, Anagnostaras SG, Sage JR, Fanselow MS, Guidotti A, Spigelman I, Li Z, DeLorey TM, Olsen RW, Homanics GE (1999) Attenuated sensitivity to neuroactive steroids in  $\gamma$ -aminobutyrate type A receptor delta subunit knockout mice. *Proc Natl Acad Sci USA* 96:12905–12910.
- Nahm WK, Noebels JL (1998) Nonobligate role of early or sustained expression of immediate early gene proteins c-Fos, c-Jun and Zif/268 in hippocampal mossy fiber sprouting. *J Neurosci* 18:9245–9255.
- Nusser Z, Mody I (2002) Selective modulation of tonic and phasic inhibitions in dentate gyrus granule cells. *J Neurophysiol* 87:2624–2628.
- Nusser Z, Hajos N, Somogyi P, Mody I (1998) Increased number of synaptic GABA<sub>A</sub> receptors underlies potentiation at hippocampal inhibitory synapses. *Nature* 395:172–177.
- Peng Z, Huang CS, Stell BM, Mody I, Houser CR (2004) Altered expression of the  $\delta$  subunit of the GABA<sub>A</sub> receptor in the mouse model of temporal lobe epilepsy. *J Neurosci* 24:8629–8639.
- Qiao X, Noebels JL (1993a) Developmental analysis of hippocampal mossy fiber outgrowth in a mutant mouse with inherited spike wave seizures. *J Neurosci* 13:4622–4635.
- Qiao X, Noebels JL (1993b) Elevated BDNF mRNA expression in the hippocampus of an epileptic mutant mouse, stargazer. *Soc Neurosci Abstr* 19:1030.
- Qiao X, Hefti F, Knusel B, Noebels JL (1998) Selective failure of brain-derived neurotrophic factor mRNA expression in the cerebellum of stargazer, a mutant mouse with ataxia. *J Neurosci* 16:640–648.
- Rouach N, Byrd K, Petralia RS, Elias GM, Adesnik H, Tomita S, Karimzadegan S, Kealey C, Bredt DS, Nicoll RA (2005) TARP $\gamma$ 8 controls hippocampal AMPA receptor number, distribution and synaptic plasticity. *Nat Neurosci* 8:1525–1533.
- Sato M, Suzuki K, Yamazaki H, Nakanishi S (2005) A pivotal role of calcineurin signaling in development and maturation of postnatal cerebellar granule cells. *Proc Natl Acad Sci USA* 102:5874–5879.

- Sieghart W, Ernst M (2005) Heterogeneity of GABA<sub>A</sub> receptors: revived interest in the development of subtype-selective drugs. *Curr Med Chem* 5:217–242.
- Sharp AH, Black III JL, Dubel SJ, Sundarraj S, Shen J-P, Yunker AMR, Copeland TD, McEnery MW (2001) Biochemical and anatomical evidence for specialized voltage-dependent calcium channel  $\gamma$  isoform expression in the epileptic and ataxic mouse, stargazer. *Neuroscience* 105:599–617.
- Sperk G, Schwarzer C, Tsunashima K, Fuchs K, Sieghart W (1997) GABA<sub>A</sub> receptor subunits in the rat hippocampus. I. Immunocytochemical distribution of 13 subunits. *Neuroscience* 80:987–1000.
- Stell BM, Brickley SG, Tang CY, Farrant M, Mody I. (2003) Neuroactive steroids reduce neuronal excitability by selectively enhancing tonic inhibition mediated by  $\delta$  subunit-containing GABA<sub>A</sub> receptors. *Proc Natl Acad Sci USA* 100:14439–14444.
- Sun C, Sieghart W, Kapur J (2004) Distribution of  $\alpha 1$ ,  $\alpha 4$ ,  $\gamma 2$ , and  $\delta$  subunits of GABA<sub>A</sub> receptors in hippocampal granule cells. *Brain Res* 1029:207–216.
- Suzuki K, Sato M, Morishima Y, Nakanishi S (2005) Neuronal depolarization controls brain-derived neurotrophic factor-induced upregulation of NR2C NMDA receptor via calcineurin signaling. *J Neurosci* 25:9535–9543.
- Thompson CL, Jalilian Tehrani MH, Barnes EM Jr, Stephenson FA (1998) Decreased expression of GABA<sub>A</sub> receptor  $\alpha 6$  and  $\beta 3$  subunits in stargazer mutant mice: a possible role for brain-derived neurotrophic factor in the regulation of cerebellar GABA<sub>A</sub> receptor expression? *Mol Brain Res* 60:282–290.
- Thompson CL, Drewery DL, Atkins HD, Stephenson FA, Chazot PL (2002) Immunohistochemical localization of *N*-methyl-D-aspartate receptor subunits in the adult murine hippocampal formation: evidence for a unique role of the NR2D subunit. *Brain Res Mol Brain Res* 102:55–61.
- Tomita S, Chen L, Kawasaki Y, Petralia RS, Wenthold RJ, Nicoll RA, Brecht DS (2003) Functional studies and distribution define a family of transmembrane AMPA receptor regulatory proteins. *J Cell Biol* 161:805–816.
- Yamada MK, Nakanishi K, Ohba S, Nakamura T, Ikegaya Y, Nishiyama N, Matsuki N (2002) Brain-derived neurotrophic factor promotes the maturation of GABAergic mechanisms in cultured hippocampal neurons. *J Neurosci* 22:7580–7585.
- Zhang Y, Mori M, Burgess DL, Noebels JL (2002) Mutations in high-voltage-activated calcium channel genes simulate low-voltage-activated currents in mouse thalamic relay neurons. *J Neurosci* 22:6362–6371.